Contents lists available at SciOpen

Food Science and Human Wellness

journal homepage: https://www.sciopen.com/journal/2097-0765

China Food Publishing Co.

Exploring biofilm-forming molecular determinants in *Listeria monocytogenes* by comparative genome-wide and transcriptomic analyses

Xinyi Zhang[a,1], Changzheng Shi[a,1], Zhaoxin Lu[a], Fanqiang Meng[a], Moutong Chen[b,*], Xiaomei Bie[a,*]

[a] *College of Food Science and Technology, Nanjing Agricultural University, Nanjing 210095, China*
[b] *Guangdong Provincial Key Laboratory of Microbial Safety and Health, State Key Laboratory of Applied Microbiology Southern China, Institute of Microbiology, Guangdong Academy of Sciences, Guangzhou 510070, China*

ARTICLE INFO

Article history:
Received 13 March 2024
Received in revised form 31 March 2024
Accepted 30 May 2024

Keywords:
Listeria monocytogenes
Biofilm
Whole genome sequencing
RNA-sequencing

ABSTRACT

In the food industry, bacterial cells usually adhere to equipment surfaces, forming biofilms that may cause persistent contamination. This study aimed to identify the key genes responsible for the stronger biofilm-forming capability of the *Listeria monocytogenes* LMB 33426 strain compared to that of the *L. monocytogenes* CICC 21662 strain through comparative genomics. Additionally, the expression of genes and related metabolic pathways of LMB 33426 and CICC 21662 strains were analyzed at the transcriptional level by high-throughput sequencing technology to uncover key differentially expressed genes between planktonic and biofilm cells of those two strains. Subsequently, the key genes found to present differences that were uncovered by those genome-wide and transcriptomic analyses were used to construct gene deletion strains. The crystalline violet assay and motility assay showed that GL002291, GL002712 and *lmo1438* genes were involved in the regulation of biofilm formation as well as motility. The hydrophobicity and auto-aggregation ability assay results demonstrated an association between the *clpB*, *lmo1438*, and *lmo0294* genes and bacterial adhesion. However, no significant differences were found regarding this association in the GL002291 and GL002712 genes. This study elucidates some potential regulatory genes associated with biofilm formation in *L. monocytogenes*, and laying a theoretical foundation for future research.

1. Introduction

Listeria monocytogenes is a foodborne pathogen that is widespread in nature. *L. monocytogenes* can cause invasive listeriosis in susceptible humans, leading to diseases such as meningitis and sepsis, with a lethality rate of up to 30%[1-3]. *L. monocytogenes* can survive and grow under a variety of conditions, such as low temperature, low pH and high sodium concentration[4]. These inherent capabilities allow the bacteria to survive and reproduce in adverse environmental conditions, which are usually present in food production facilities[5]. Studies have shown that the persistence of bacterial contamination is usually related to the existence of biofilm[6]. Extracellular polymeric substances (EPS) provide the biofilm with a steady structure that enhances the tolerance of bacterial cells to detergents and disinfectants, posing a serious risk to food safety[7]. In the food industry, uncovering the mechanisms of biofilm formation and finding ways to control the formation of *L. monocytogenes* biofilm are important aspects in preventing its contamination[8].

Whole genome sequencing (WGS) can achieve the tracing of pathogens and provide abundant molecular information of the sequenced strains[9]. WGS is a vital method for identifying key factors within bacterial genomes and exploring the mechanisms of persistent

[1] These authors contribute equally to this work.
[*] Corresponding authors.
E-mail address: bxm43@njau.edu.cn (X.M. Bie); cmtoon@hotmail.com (M.T. Chen)
Peer review under responsibility of Beijing Academy of Food Sciences.

SciOpen Publishing services by Tsinghua University Press

http://doi.org/10.26599/FSHW.2024.9250297

bacterial contamination. For example, Unrath et al.[10] found that the terminal codon mutation of *inlA* causes the inactivation of the internalin protein by utilizing the WSG, leading to a decrease in the virulence of *L. monocytogenes*. Comparative genomics is the study of genetic similarities and differences among different organisms, which plays a crucial role in predicting potential genes and facilitating the elucidation of gene regulatory mechanisms. Casey et al.[11] demonstrated the importance of accessory genes in pathogenesis through a comparative genomic analysis of two *L. monocytogenes* strains with different infectivity levels. The genome sequences of the pathogenic strains EGD-e and F2365 of *L. monocytogenes* were compared to the non-pathogenic strains *L. innocua* CLIP1182 and *L. monocytogenes* HCC23. The results revealed a set of genes present only in the pathogenic strain. These genes were shown to play a role in the pathogenicity of *L. monocytogenes* by constructing gene mutant strains and measuring their adhesion and ability to infect the liver and spleen of mice[12]. Comparative genomics may facilitate the identification of specific genes found in strains that exhibit increased abilities in biofilm formation. In this way, it is hoped that comparative genomics will contribute to a deeper understanding of the molecular mechanisms involved in biofilm formation.

In order to get rid of biofilms, it is crucial to reveal the regulation of their synthesis and maintenance. The application of transcriptomic studies is essential for elucidating the genetic mechanism of this process[13]. Luo et al.[14] found that the differentially expressed genes between the planktonic and biofilm states cover most of the biochemical functions within bacterial cells through analyzing the gene expression profiles of *L. monocytogenes*, indicating that the biofilm formation of *L. monocytogenes* is regulated by a complex network. Rodríguez-Melcón et al.[15] identified the gene *lbrA*, which potentially plays a regulatory role in biofilm formation, through comparative transcriptome analysis of strong and weak biofilm forming strains of *L. monocytogenes*. Sequencing of differential biofilm-forming strains by RNA-seq allows systematic comparison of metabolic pathways between strains. This approach serves as a theoretical basis for the subsequent development of novel biofilm eradicating methods.

In this study, we uncovered the whole genome of *L. monocytogenes* LMB 33426 and CICC 21662 strains with significant differences in biofilm forming. Moreover, transcriptome analysis was conducted on both the LMB 33426 and CICC 21662 strains in both biofilm and planktonic states. We then analyzed the results to detect those genes closely related to biofilm formation. Then, we constructed the corresponding gene deletion mutant strains and determined some of their biological properties related to biofilm formation. Altogether, we have illustrated some of the molecular determinants (genes) seemingly involved in the biofilm formation process, which contribute to reducing the risk of biofilm contamination in the food industry.

2. Materials and methods

2.1 Strains and plasmids

L. monocytogenes strains LMB 33426 and FSIS 57034 were maintained in our laboratory. ATCC 19116 strain was purchased from the American Type Culture Collection. CICC 21662 strain was purchased from the China Center of Industrial Culture Collection. *Escherichia coli* JM109 and JM110 (Vazyme, Nanjing, China) were utilized as host strains of plasmid pKSV7 for the cloning experiments. Single colonies were selected after rejuvenation and inoculated into sterile liquid seed broth for preparing bacterial suspensions before use. All strains used in this study were cultured in Luria-Bertani (LB) medium, which consists of tryptone 1 g, yeast extract 0.6 g, NaCl 0.5 g/100 mL, at 37 ℃.

2.2 Determination of biofilm formation ability of L. monocytogenes

Quantitative analysis of the biofilm was performed using crystalline violet staining, following a previous method with minor modifications[16]. *L. monocytogenes* strains were cultured in LB medium at 37 ℃ for 12 h, and the $OD_{595\,nm}$ of the bacterial solution was adjusted to 0.50 ± 0.02. Subsequently, 1% of the inoculum was transferred into LB medium, with 200 μL per well in a 96-well plate. Three replicates were performed for each strain. After incubating at 37 ℃ for 12, 24, 36, 48, 60 and 72 h, the medium was discarded, and the wells were washed three times with 200 μL of phosphate buffered saline (PBS). After drying, 200 μL of 0.1% crystalline violet solution was added to each well for 30 min. Afterwards, the floating crystalline was washed three times with PBS. The wells were air-dried, and 200 μL of 95% (*V*/*V*) ethanol were added to each well to dissolve the crystalline violet. The absorbance of the sample was measured at 595 nm by a microplate reader (Ensight, PerkinElmer, USA) after 15 min at room temperature.

Confocal laser scanning microscopy (CLSM) was performed following a previous method with minor modifications[17]. The 2 mL of broth was added into sterile glass bottom dish (Cellvis, Mountain View, USA). The inoculated broths were then cultivated at 37 ℃ for 36 h after inoculating with 1% seed broth of *L. monocytogenes*. The glass bottom dish was washed with sterile PBS and stained with 20 mmol/L SYTO 9 and propidium iodide (PI) at room temperature for 30 min in the dark. The images were captured by CLSM using a 40× oil-immersion lens with 488 nm settings for the green signal, and 630 nm settings for the red signal.

2.3 Determination of hydrophobicity and auto-aggregation of L. monocytogenes

2.3.1 Cell surface hydrophobicity

The cell surface hydrophobicity was determined using a minor modified BATH test[15]. *L. monocytogenes* strains were inoculated into LB liquid medium and incubated at 37 ℃ for 24 h. The bacterial solution was centrifuged at 10 000 × *g* for 5 min, and the supernatant was discarded. After being washing twice, the pellet was resuspended in a 0.1 mol/L PBS and its $OD_{540\,nm}$ value of the resulting suspension was adjusted to 0.90 ± 0.05 and recorded as OD_0. For every 4 mL of sample, 1 mL of xylene was added, shaken vigorously for 2 min, and then allowed to stand for 30 min at 37 ℃. After the system separated, the OD of the lower aqueous phase at 540 nm was measured and recorded as OD_1. Thus, the cell surface hydrophobicity was calculated using the following equation (1):

$$\text{Cell surface hydrophobicity (\%)} = \frac{OD_0 - OD_1}{OD_0} \times 100 \quad (1)$$

2.3.2 Auto-aggregation ability

L. monocytogenes strains were inoculated into LB medium at 1% inoculum. Auto-aggregation ability was measured using the previously described method[18]. After 24 h, cells were collected by centrifugation. The bacterial cells were washed three times with 0.1 mol/L PBS at pH 7.4. The bacteria were resuspended in the same buffer and the $OD_{600\,nm}$ of each bacterial suspension was adjusted to approximately 0.8 and recorded as A_0. The bacterial supernatant was incubated at 37 ℃ for 6 h. An equal amount of supernatant of each strain was combined and its $OD_{600\,nm}$ was measured and recorded as A_1. The experiment was repeated three times. The auto-aggregation ability of each strain was calculated according to the following equation (2):

$$\text{Auto-aggregation ability}\ (\%) = \frac{A_0 - A_1}{A_0} \times 100 \quad (2)$$

2.4 Determination of motility of L. monocytogenes

2.4.1 Morphological observation of flagella

The LMB 33426 and CICC 21662 strains were cultured on LB agar plates at 30 ℃ for 18 h. After incubation, individual colonies were selected and dispersed in deionized water to create suspensions. These suspensions were then fixed onto copper sheets and subjected to negative staining using an anionic dye. Subsequently, the flagellar growth of both *L. monocytogenes* strains was observed using HT-7700 transmission electron microscopy after the samples were dried.

2.4.2 Determination of swimming ability

Swimming ability was determined according to previous method with minor modifications[19]. *L. monocytogenes* strains were cultured to log phase, and then inserted into semisolid plates using a sterile inoculation needle. These plates containing 1.0 g/100 mL trypsin, 0.5 g/100 mL NaCl and 0.3 g/100 mL agar for swimmer agar plates or 0.5 g/100 mL agar for cluster agar plates. These plates were incubated at 30 or 37 ℃ for 24 h, because *L. monocytogenes* exhibits different flagellar characteristics at the 2 temperatures. The bacteria migrated from the center to the periphery of the plate through the agar. The diameter of the migration zone was measured using a vernier caliper.

2.5 WGS

The LMB 33426 and CICC 21662 strains were picked into LB broth and incubated at 37 ℃ with shaking (180 r/min) until $OD_{600\,nm}$ reached 0.5–0.6. The microorganisms were collected through centrifugation, washed three times with PBS. Subsequently, genomic DNA extraction was performed according to the instructions of bacterial genome extraction kit (Omega Bio-tek, Inc., USA). The WGS of *L. monocytogenes* LMB 33426 and CICC 21662 was executed at BGI Genomics (Shenzhen, China).

We used the MEGA11 software to construct the phylogenetic tree. Sequences were aligned using ClustalW and refined for accuracy. The maximum likelihood method in MEGA11 was employed for tree construction, along with bootstrap analysis consisting of 1 000 replicates for assessing tree reliability.

2.6 RNA-Seq

The bacteria were cultured in 6-well plates, and the bacterial suspension was centrifuged to collect planktonic cells. Subsequently, the 6-well plates were washed with sterilized PBS to remove any unattached cells. The biofilm adhering to the 6-well plates was collected, and the cells in the biofilm state were then centrifuged to obtain them. Total RNA was extracted from LMB 33426 and CICC 21662 cells in biofilm and planktonic states, respectively, after 36 h of incubation at 37 ℃. The TransZol Up® RNA kit was used for extraction (TransGen Biotech, Beijing, China). The transcriptome sequencing of both strains was provided by UW Genetics in Shenzhen.

2.7 Construction of deletion and complement strains of key regulatory genes in L. monocytogenes

The construction of mutant strains was performed according to previous method. The genomic DNA was extracted from *L. monocytogenes* LMB 33426 using the MicroElute Genomic DNA kit (Omega Bio-Tek, USA). Polymerase chain reaction (PCR) amplification of *L. monocytogenes* genes was performed using 2× Phanta Max Master Mix (Vazyme, Nanjing, China) and specific primers. All primers used for mutant construction are listed in Table 1. The upstream and downstream homologous arms of each target gene were amplified by PCR using primer pairs F1/R1 and F2/R2, respectively. Primer F1/R2 was used to fuse the upstream and downstream fragments by gene splicing by overlap extension (SOE) PCR. The fusion fragments were ligated into the temperature-sensitive shuttle vector pKSV7 using the ClonExpress II One Step Cloning kit (Vazyme, Nanjing, China). The recombination plasmids were transferred into *E. coli* JM109 and JM110 successively by heat shock to obtain the unmethylated plasmids. The unmethylated recombination plasmids were transferred into LMB 33426 competent cells by electroporation. The homologous recombination was undergone with dual pressure of chloramphenicol and temperature. DNA sequencing was used to further confirm the sequences of the mutant strains. For gene complementation, the full-length gene and its upstream and downstream sequences were amplified from genomic DNA by PCR using primer pair F1/R2. The amplified fragments were cloned into the vector pKSV7 using the ClonExpress II One Step Cloning kit and transformed into JM109 and JM110 competent cells. Subsequently, the construction of complement strains was carried out according to the above method of gene knockout, and verification was conducted by PCR.

2.8 Statistical analysis

All of the above experiments were conducted in triplicate, and all values are expressed as the means ± standard deviations (SD). Data were analyzed using ANOVA, followed by Duncan's test and Student's *t* test to determine the significant difference between the means using SPSS 20.0 software. $P < 0.05$ was considered statistically significant.

Table 1
Primers used for gene knockout and complementation.

Primer	Sequence (5′-3′)	Purpose
GL002291-F1	CCAAGCTTGCATGCCTGCAGGTTGTTTGGCAAGTTATCCGG	Amplification of GL002291 upstream homologous arms
GL002291-R1	AAAACAATGTAGAATTAATTGTTTGAAGGAGTGAGAGGTATGA	
GL002291-F2	AATTAATTCTACATTGTTTTCGTTTAAAAACTGGCGCATT	Amplification of GL002291 downstream homologous arms
GL002291-R2	TTGTGTGGAATTGTGAGCGGTGAATGCTTTTGTTTACTGCG	
GL002712-F1	CCAAGCTTGCATGCCTGCAGCATTTGGCAATTCCATTCTCCAG	Amplification of GL002712 upstream homologous arms
GL002712-R1	TGTAATTTTTTAATTTAGTTGCAAAAAAGACAATAGGCACG	
GL002712-F2	AACTAAATTAAAAAATTACAGAGTCGATTTCCTAATTCAGGC	Amplification of GL002712 downstream homologous arms
GL002712-R2	TTGTGTGGAATTGTGAGCGGTGGTCTATGGTCTGAAATAAATTCG	
clpB-F1	GTCGACCGCTAATTCCTTCTAGGAATTTCAC	Amplification of *clpB* upstream homologous arms
clpB-R1	TTTATAAGGAGGACGAATGACATAGAAAAGGTTTGACACCTCA	
clpB-F2	TCATTCGTCCTCCTTATAAAAGATAAGTCTGACCTTTTTTGACC	Amplification of *clpB* downstream homologous arms
clpB-R2	GAGCTCCGATTGGGAGTAAATTAAGTCCAG	
lmo1438-F1	GAGCTCCGATAATACGATTTAAGCCAAATGC	Amplification of *lmo1438* upstream homologous arms
lmo1438-R1	GAAAAGTGAGGTAACTATGCTCAAAAACCACTTTCATTTATGTGAA	
lmo1438-F2	GCATAGTTACCTCACTTTTCAATAATACCTTTCCCTATTGTAGCTG	Amplification of *lmo1438* downstream homologous arms
lmo1438-R2	GTCGACAACTATGGAAATTCACTATACAAAGC	
lmo0294-F1	CCAAGCTTGCATGCCTGCAGCAAGAGACTCAGCAGCAATAAC	Amplification of *lmo0294* upstream homologous arms
lmo0294-R1	AATTTTCTCCTTTTGGTATCAAAAATAATGATACCGGCATATGA	
lmo0294-F2	ATACCAAAAGGAGAAAATTGTTGTTGATTACAACCCTTTCAAG	Amplification of *lmo0294* downstream homologous arms
lmo0294-R2	TTGTGTGGAATTGTGAGCGGCCAAATTGTAACGGTCGGGA	
pKSV7-F	CCGCTCACAATTCCACACAAC	Inverse PCR to linearize plasmid pKSV7
pKSV7-R	CTGCAGGCATGCAAGCTTG	

3. Results

3.1 Biofilm formation ability of L. monocytogenes

We quantified the biofilm-forming capacity of 4 *L. monocytogenes* strains using crystal violet staining. As shown in Fig. 1A, LMB 33426 had the strongest biofilm-forming capacity, followed by FSIS 57034 and ATCC 19116 strains, while CICC 21662 showed the weakest biofilm-formation. The most significant difference in biofilm formation ability was observed between LMB 33426 and CICC 21662 strains. Additionally, CLSM experiments were performed on four strains of *L. monocytogenes*. The results showed that LMB 33426 forms a thicker and more evenly distributed biofilm, while CICC21662 forms a smaller amount of biofilm with more voids (Fig. 1B). The LMB 33426 and CICC 21662 strains were selected for further experiments, including determination of cell surface hydrophobicity, auto-aggregation, comparative genomic analysis, and comparative transcriptomic analysis.

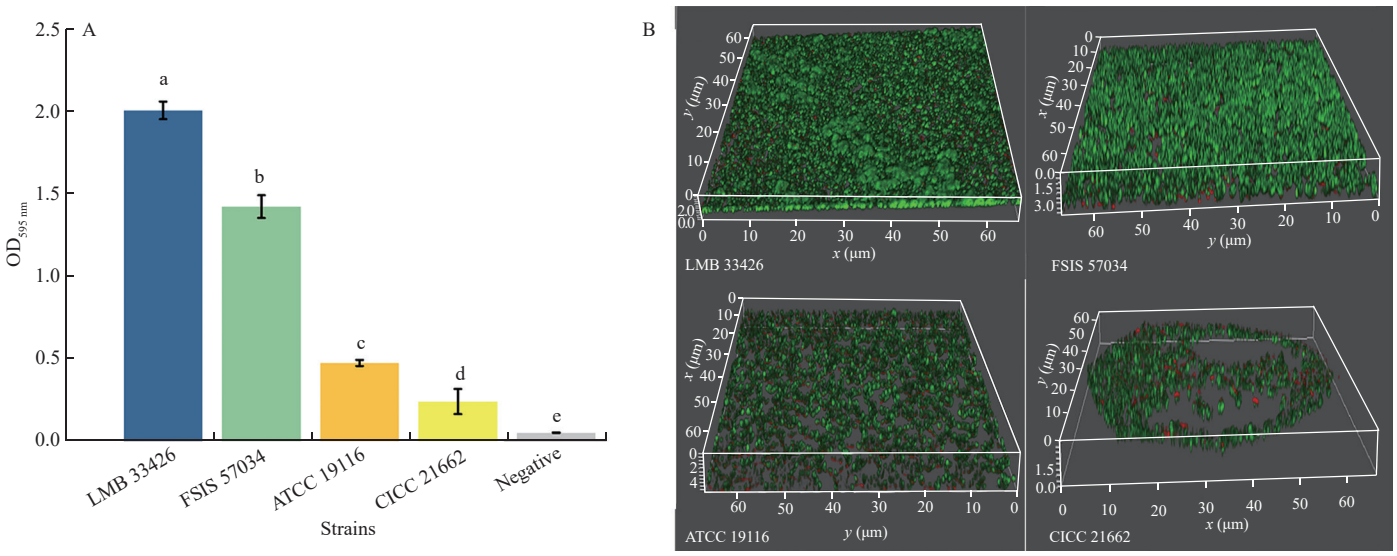

Fig. 1 Biofilm formation ability of four different *L. monocytogenes* strains. (A) $OD_{595\ nm}$; (B) CLSM images. Different lowercase letters mean statistical significance ($P < 0.05$).

3.2 Cell surface hydrophobicity and auto-aggregation ability of L. monocytogenes

The cell surface hydrophobicity and auto-aggregation ability were measured to evaluate the cell surface characteristics. The results in Fig. 2 showed that there is no significant difference in the cell surface hydrophobicity and auto-aggregation abilities between LMB 33426 and CICC 21662. The results demonstrated that both LMB 33426 and CICC 21662 exhibit similar cell surface characteristics.

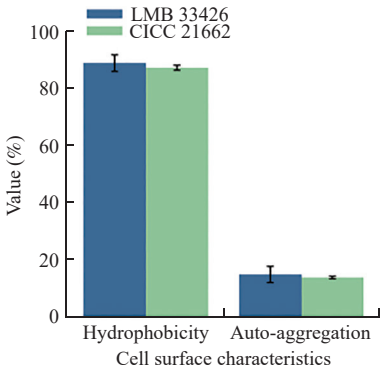

Fig. 2 Cell surface hydrophobicity and auto-aggregation of LMB 33426 and CICC 21662 strains.

3.3 Motility of L. monocytogenes

The flagellar morphology of the two strains was observed separately under transmission electron microscopy as shown in Figs. 3A and B. It was found that LMB 33426 possesses multiple circumferential flagella, which appear as wavy curved filaments. The circumferential flagella contribute to the motility of the LMB 33426. However, CICC 21662 did not form any flagella around it. Furthermore, the motility ability of LMB 33426 and CICC 21662 was evaluated using the semisolid plate method at 30 and 37 °C. Figs. 3C and D show that the LMB 33426 forms uniform diffusion circles on the semisolid plate, while CICC 21662 does not diffuse on the semisolid plate at both 37 and 30 °C.

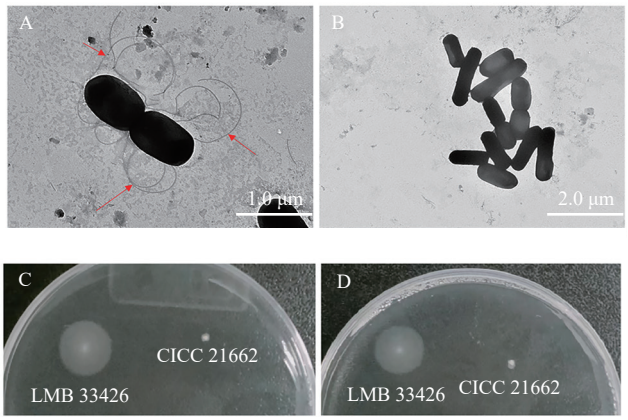

Fig. 3 Motility ability of LMB 33426 and CICC 21662 strains. Transmission electron micrographs of (A) LMB 33426 flagella and (B) CICC 21662 flagella. Motility capacity at (C) 37 and (D) 30 °C.

3.4 Results of WGS

3.4.1 Data processing and genome assembly

After second-generation sequencing, both LMB 33426 and CICC 21662 obtained 8 764 210 reads. The original data size was 1 314 Mb and a clean data size of 1 307 Mb available after data filtering. For the original data from third-generation sequencing, LMB 33426 obtained 184 594 reads with an average length of 13 900. CICC 21662 obtained 172 458 reads with an average length of 17 395. Based on the valid data from the second- and third-generation sequencing platforms, the whole genome circle maps of the assembled sequenced samples are shown in Fig. 4. The distribution of genes, ncRNAs, annotations, and other data results were displayed on the genome to show the distribution of each component.

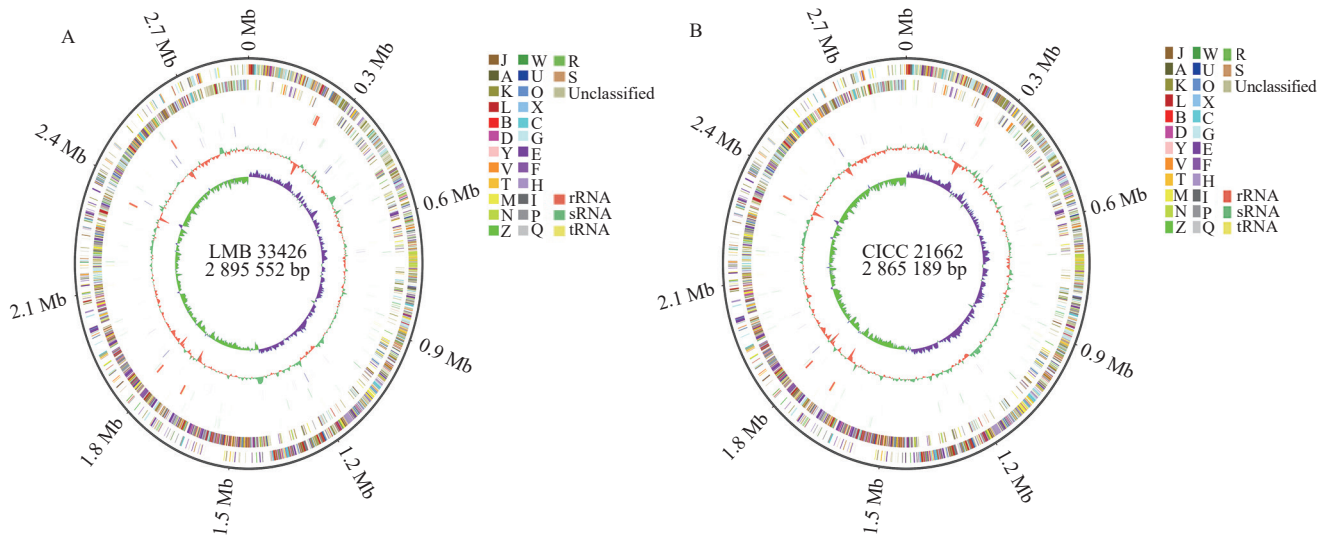

Fig. 4 The circular map of the (A) LMB 33426 and (B) CICC 21662 genomes. From outer to inner, the 1st circle indicates genome size; the 2nd circle indicates forward strand gene, colored according to Cluster of Orthologous Groups (COG) classification; the 3rd circle indicates reverse strand gene, colored according to COG classification; the 4th circle indicates forward strand ncRNA; the 5th circle indicates reverse strand ncRNA; the 6th circle indicates GC content; the 7th circle indicates GC-skew value.

3.4.2 Genomic component analysis

After completing the sequence assembly, the genome components were analyzed and the basic sequence characteristics of the genomes of samples LMB 33426 and CICC 21662 are shown in Table 2. The results showed that the genome size of LMB 33426 is 30 363 bp larger than that of CICC 21662, and LMB 33426 has more genes than CICC 21662.

Table 2
Basic characteristics of LMB 33426 and CICC 21662 genomes.

Item	LMB 33426	CICC 21662
Genome size (bp)	2 895 552	2 865 189
Gene number	2 847	2 806
Gene average length (bp)	901	908
Gene length in the total genome length (%)	88.54	88.94
GC content (%)	38.63	38.56
tRNA	67	67
16S/23S/5S rRNA	6	6
sRNA	102	99

The bioinformatic analysis revealed that both LMB 33426 and CICC 21662 contained prophage sequence information (Table 3). LMB 33426 possessed 13 prophages, named LPP, and CICC 21662 possessed 11 prophages, named CPP. Similarity analysis (NCBI nucleotide blast) of the prophage sequences of the 2 strains showed that seven pairs of prophage sequences had similarity. Notably, LPP3 was a prophage of LMB 33426 with a sequence length of 38 517 bp containing 46 genes, which most of them were motility-related genes. The sequence of prophage CPP5 in CICC 21662 had a sequence length of 43 326 bp and contained 51 genes, which was found to be 93.66% similar to the LPP3. The LPP3 and CPP5 sequences were compared using NCBI database (Standard Nucleotide BLAST program) to evaluate the motility related genes. The results showed that the motility genes in LMB 33426 and CICC 21662 were mostly consistent. However, only the flagellar biosynthetic protein genes *fliP*, *fliQ*, *fliR*, and the thiamine pyrophosphate-requiring enzyme were present in CICC 21662 (Table S1). The results indicated that the difference in motility capacity could be associated with the difference in flagellar related genes.

Table 3
Sequence similarity analysis of prophages between LMB 33426 and CICC 21662.

LMB 33426 ID	Length (bp)	CICC 21662 ID	Length (bp)	Coverage (%)	Similarity (%)
LPP1	65 260	CPP3	43 344	66	96.18
LPP2	15 951	–		–	–
LPP3	38 517	CPP5	43 326	98	93.66
LPP4	30 478	CPP6	29 619	94	95.23
LPP5	43 466	CPP8	47 377	99	95.30
LPP6	12 836	–		–	–
LPP7	15 718	–		–	–
LPP8	20 863	CPP9	22 542	93	93.92
LPP9	11 639	CPP10	6 410	100	93.20
LPP10	6 644	–		–	–
LPP11	40 394	CPP11	50 787	90	96.93
LPP12	27 131	–		–	–
LPP13	14 754	–		–	–

Note: LPP represents the prophage sequence present in strain LMB 33426; CPP represents the prophage sequence present in strain CICC 21662; – represents no match to a similar sequence.

3.4.3 Gene function analysis

The WGS of LMB 33426 and CICC 21662 were compared to the Clusters of Orthologous Groups (COGs; https://www.ncbi.nlm.nih.gov/research/COG), Gene Ontology (GO; http://www.geneontology.org) and Kyoto Encyclopedia of Genes and Genomes (KEGG; http://www.genome.jp/kegg/) databases for annotation. We classified the genes of LMB 33426 and CICC 21662 based on the COGs. As shown in Fig. 5, the differences in COG classification between LMB 33426 and CICC 21662 were not significantly concentrated in one classification. The data presented that out of the 2 847 genes involved in encoding proteins in LMB 33426, 2 305 genes could be matched to the COG classification, accounting for 80.96% of all genes. For CICC 21662, out of the 2 806 genes encoding proteins, 2 355 genes could be matched to the COG classification, accounting for 83.93% of all genes. Overall, the functional classification with the highest percentage of known coding genes in both LMB 33426 and CICC 21662 was carbohydrate transport and metabolism, followed by transcription-related functions. Both LMB 33426 and CICC 21662 possessed the pathways probably associated with biofilm formation, which included the cell motility, cell wall/membrane/envelope biogenesis and extracellular structure pathways. At the cellular level, both LMB 33426 and CICC 21662 contained 41 cell motility genes and 6 extracellular structure-related genes. Additionally, LMB 33426 had 125 genes related to cell wall/membrane/envelope biogenesis, while CICC 21662 had 132 genes associated with the same functional category.

The results of GO annotation showed that the genes of LMB 33426 and CICC 21662 were mainly involved in cellular processes and metabolic processes (Fig. 6). It was observed that LMB 33426 contained 7 genes related to bio-adhesion and 331 genes related to localization, while CICC 21662 contained 8 and 343 genes related to bio-adhesion and localization respectively. The bio-adhesion and localization related genes should be associated with the formation of biofilm. Additionally, the LMB 33426 had 104 genes associated with response to stimulus, while CICC 21662 had 107 genes. In terms of molecular function, the annotated genes were mostly involved in binding and catalytic activities.

Using the KEGG database, the annotated genes of LMB 33426 and CICC 21662 were classified into six categories, namely, cellular processes, environmental, genetic, human diseases, metabolism, organismal system, based on the KEGG metabolic pathway (Fig. 7). The data showed that 1 842 genes were functionally classified, accounting for 64.70% of all genes. On the other hand, out of the 2 806 protein-coding genes in CICC 21662, a total of 1 903 genes were functionally classified, accounting for 67.82% of all genes. Overall, the functional classifications with the highest proportion of known coding genes in both LMB 33426 and CICC 21662 were global and overview maps (a secondary category under the metabolism, which displays the relationships between various biological processes and pathways), followed by carbohydrate metabolism. Both LMB 33426 and CICC 21662 had 33 genes annotated to cell motility, and LMB 33426 had 6 genes annotated to environmental adaption, while CICC 21662 had 7 genes annotated to environmental adaption.

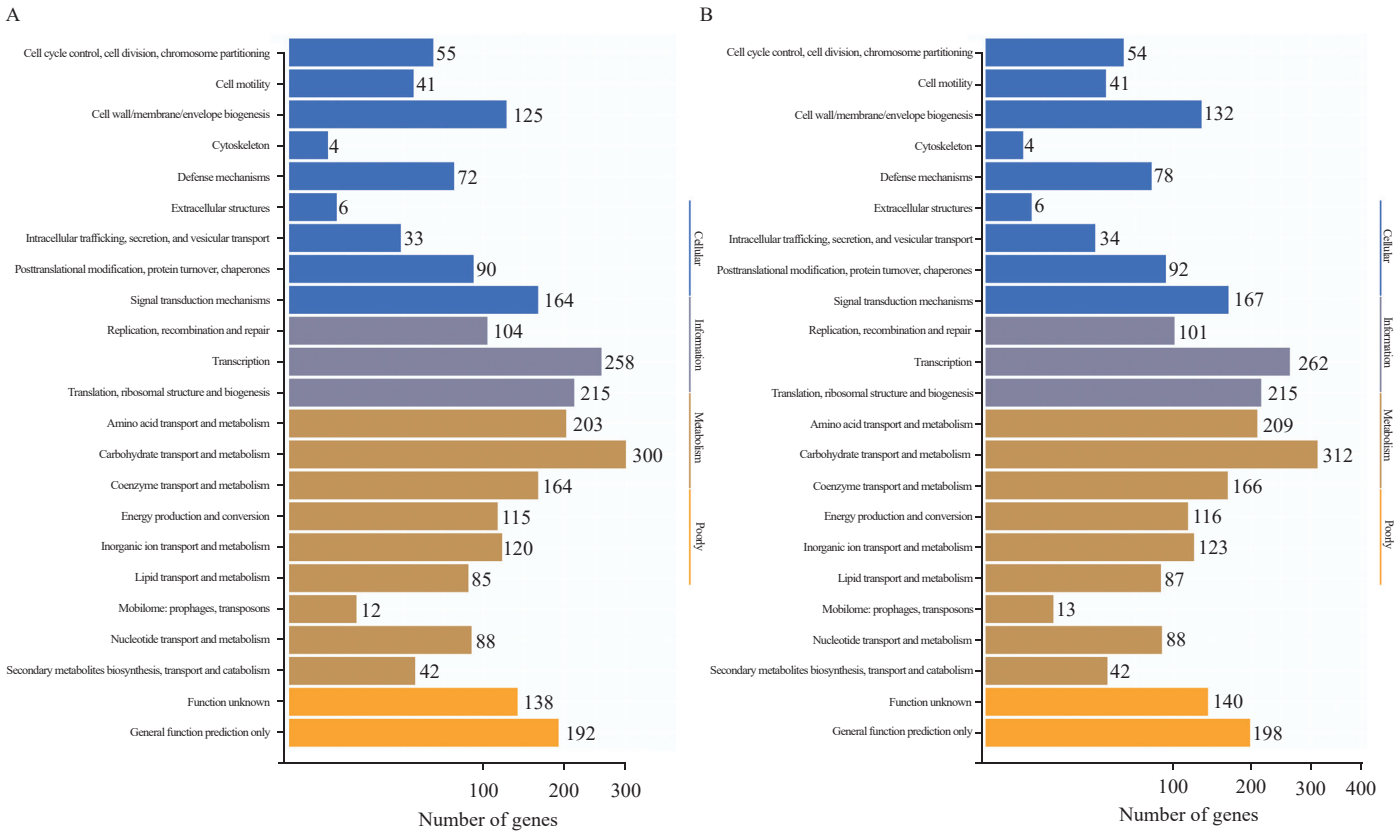

Fig. 5 COG annotation of (A) LMB 33426 and (B) CICC 21662.

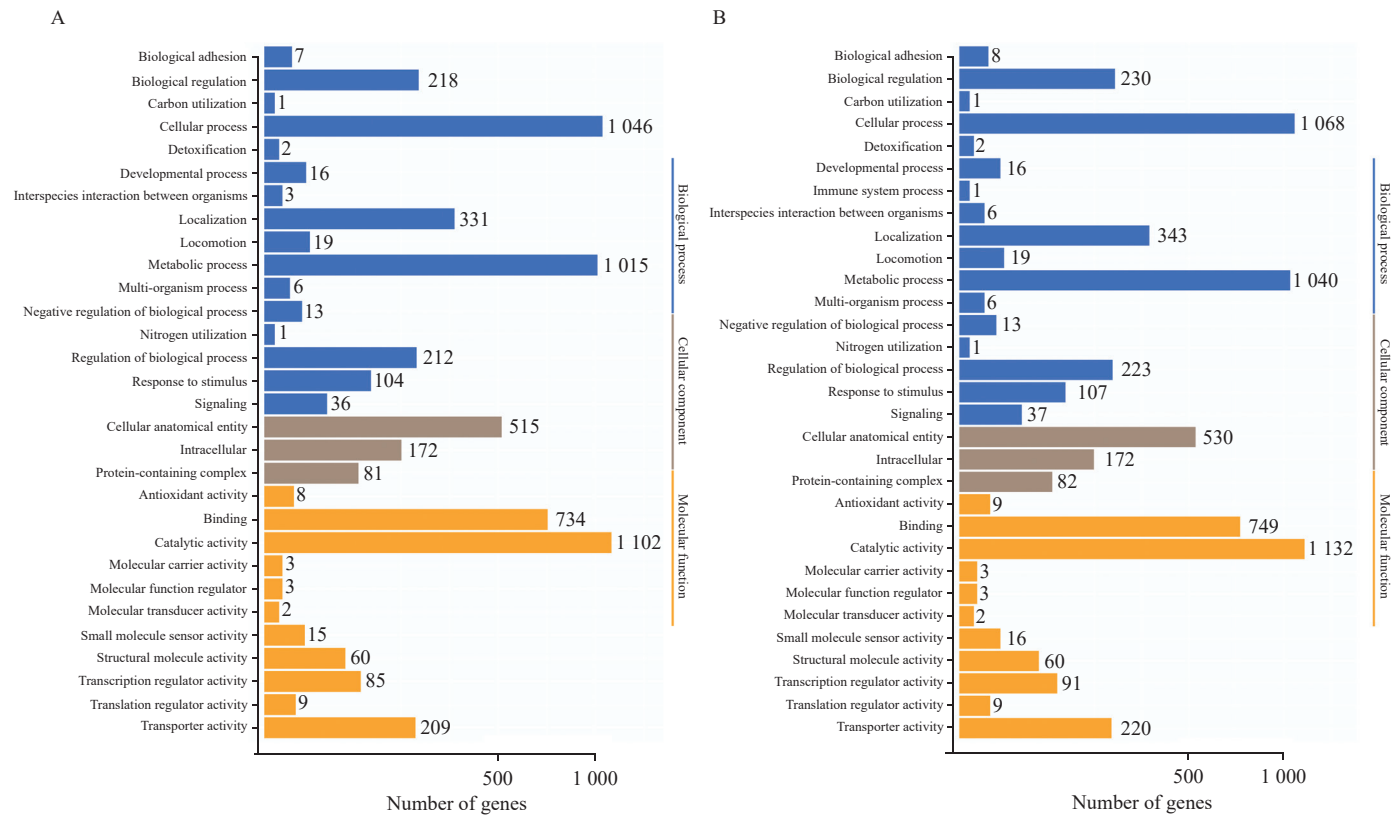

Fig. 6 GO annotation of (A) LMB 33426 and (B) CICC 21662.

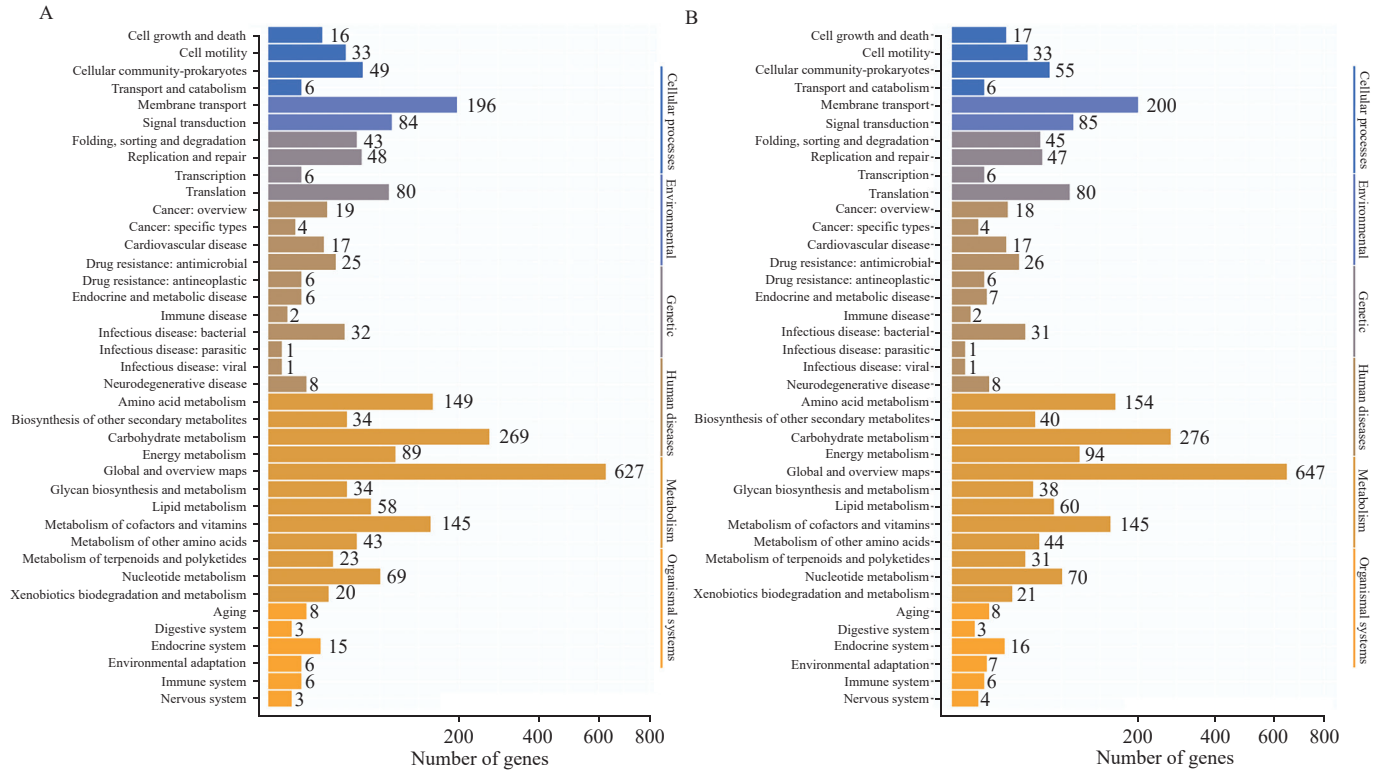

Fig. 7 KEGG annotation of (A) LMB 33426 and (B) CICC 21662.

3.5 Comparative genomic analysis

3.5.1 Analysis of motility genes

The previous results (Section 3.4.2) indicated that motility-related genes present in LMB 33426 were also found in CICC 21662 (Table S1). We supposed that the sequence information of some key genes related to flagellar formation was mutated or not expressed, resulting in different motility phenotypes. We tried to identify the potential regulatory genes related to motility differences between LMB 33426 and CICC 21662. The results showed that some genes related to motility in CICC 21662 had different lengths compared to those of LMB 33426 (Table 4). Additionally, the flagellar assembly system is illustrated in Fig. S1, with genes depicted in blue highlighting the differences between LMB 33426 and CICC 21662. Both GL001051 of LMB 33426 and GL001093 of CICC 21662 encoded the flagellar-specific peptidoglycan hydrolase FlgJ. However, the length of GL001051 was longer by 399 bp than GL001093. LMB33426 GL000675 and CICC21662 GL000691 both belong to MogR-encoded genes, which differ by 174 bp in length. Additionally, LMB33426 GL000677 and CICC21662 GL000693 both encode FliP proteins, which differ in length by 108 bp. These mutated flagellar synthesis-related genes may be one of the factors contributing to the differences in flagellar motility between LMB 33426 and CICC 21662.

Table 4
Motility-related genes of LMB 33426 and CICC 21662 strains.

LMB 33426 fragment name	CICC 21662 fragment name	Gene	Gene length difference (bp) (LMB 33426 *vs.* CICC 21662)
GL000675	GL000691	*mogR*	174
GL000677	GL000693	*fliP*	108
GL000686	GL000702	*motA*	24
GL000693	GL000709	*cheA*	27
GL000706	GL000722	*flgK*	36
GL000707	GL000723	*flgL*	–3
GL000715	GL000731	*fliG*	–6
GL001051	GL001093	*flgJ*	399
GL001165	GL001215	*bax*	–42
GL001166	GL001216	*bax*	27
GL001312	GL001348	*comGD*	–6
GL002405	GL002405	*rpoN*	81
GL002545	GL002540	Unknown gene	–12
GL002648	GL002645	*cwlS*	3

3.5.2 Genomic collinearity analysis

Collinearity analysis is an indispensable analysis strategy for comparatively analyzing genomes. The results showed that LMB 33426 exhibited the lowest sequence similarity with the CICC 21662 at 89.68% (Table 5). The CICC 21662 showed a high degree of similarity to the known WGS of *L. monocytogenes* EGD-e (98.16%) and *Lm*.10 (98.16%). In contrast, the sequence similarity between LMB 33426 and *L. monocytogenes* EGD-e is only 90.21%. The data indicated that the potential occurrence of structural variations in the genomes of LMB 33426 and CICC 21662 during the evolutionary process.

Table 5
Structural variations analysis of LMB 33426 and CICC 21662 at the nucleotide level through collinearity.

Group	Similarity (%)
LMB 33426 *vs. Lm*. 10	90.25
LMB 33426 *vs. Lm*. 11	91.08
LMB 33426 *vs. Lm*. 52873	94.77
LMB 33426 *vs. Lm*. EGD-e	90.21
LMB 33426 *vs. Lm*. UKVDL7	94.56
LMB 33426 *vs.* CICC 21662	89.68
CICC 21662 *vs. Lm*. 10	98.16
CICC 21662 *vs. Lm*. 11	96.41
CICC 21662 *vs. Lm*. 52873	92.13
CICC 21662 *vs. Lm*. EGD-e	98.16
CICC 21662 *vs. Lm*. UKVDL7	91.23

3.5.3 Distinctive genes analysis

The phylogenetic tree allows for visualizing the evolutionary relationships among species, with the length of the line segment representing the evolutionary distance. Compared to CICC 21662, LMB 33426 has a more distant genetic relationship with the standard strain EGD-e, indicating that LMB 33426 may have undergone more evolution to adapt to the environment (Fig. 8).

According to the whole-genome data, both LMB 33426 and CICC 21662 possess their endemic genes. The results showed that there was a total of 140 endemic genes in LMB 33426 and 47 endemic genes in CICC 21662 (Data not shown). Based on COG annotation, LMB 33426 possessed only one endemic gene GL002712, which belongs to the cell wall/membrane/envelope biogenesis pathway. In addition, the COG annotated endemic genes revealed that LMB 33426 GL002291 was present in multiple pathways, including carbohydrate transport and metabolism, transcription and signal transduction mechanisms. Therefore, we selected the deletion of GL002712 and GL002291 genes in LMB 33426 for functional validation.

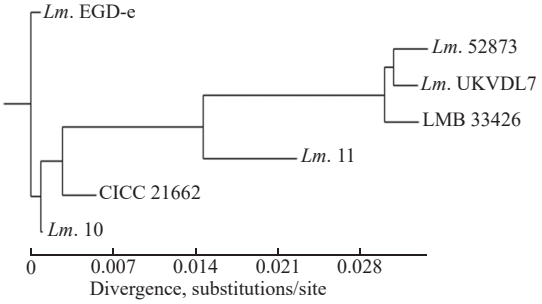

Fig. 8 Analysis of phylogenetic tree.

3.6 Analysis of transcriptome

The significantly enriched differentially expressed genes in the biofilm and planktonic states of LMB 33426 were analyzed in the previous study (the data have not been published) and subsequently validated through RT-qPCR (Fig. S3). The *clpB* gene encodes an ATPase and a penicillin-binding protein, playing a role in regulating stress response, motility, and biofilm formation. Additionally, the *lmo1438* exhibited the highest expression level among the penicillin protein encoding genes. Furthermore, the gene expression difference in the biofilm state of LMB 33426 and CICC 21662 was analyzed. The results showed that the expression level of *lmo0294* in LMB 33426 was higher than in CICC 21662. The *lmo0294* is associated with the transcriptional regulatory pathway (Table 6). Therefore, *clpB*, *lmo1438* and *lmo0294* genes were selected for biofilm validation experiments.

3.7 The effect of key genes on biofilm formation

We supposed that GL002291, GL002712, *clpB*, *lmo1438*, and *lmo0294* are involved in the key biofilm related genes. We successfully constructed GL002291, GL002712, *clpB*, *lmo1438*, and *lmo0294* mutant strains and their complement strains (Fig. S2).

The capacity of biofilm formation was determined using crystalline violet staining. The results showed that ΔGL002291, ΔGL002712, Δ*clpB*, Δ*lmo1438*, and Δ*lmo0294* gene deletion mutant strains exhibited a significantly decrease of biofilm capacity compared to wild type (WT) ($P < 0.05$). The biofilm formation

Table 6
Differentially expressed genes of BF_CICC 21662 and BF_LMB 33426, P_LMB 33426 and B_LMB 33426.

Gene	Function	$\log_2$ Fold change	
		BF_CICC 21662 *vs.* BF_LMB 33426	P_LMB 33426 *vs.* BF_LMB 33426
lmo0294	Transcriptional regulatory	9.76	1.53
carB	Large subunit of carbamyl phosphate synthase	5.61	2.98
lmo1799	Neuroblastoma amplification sequence	5.44	1.24
lmo1837	Allantoinase	5.30	3.34
lieB	ATP binding box A subgroup (ABCA1)	4.92	2.68
clpB	Clp protease submit B	–	2.15
lmo1438	Putative penicillin-binding protein	–	5.15

Note: BF represents cells in the biofilm state, P represents cells in the planktonic state; – means no differential expression genes were found.

capacity was restored in complementary strains (Fig. 9). The results demonstrated that GL002291, GL002712, *clpB*, *lmo1438*, and *lmo0294* genes regulated biofilm formation in *L. monocytogenes*. At the 12 h incubation, the biofilm formation capacity of gene deletion strains showed a significant decrease compared to the WT. The most significant difference in biofilm formation between the WT and mutant strains was observed after 24 h of cultivation. Compared to WT, the biofilm formation capacity decreased by 23% and 28.23% for the ΔGL002291 and ΔGL002712 gene deletion strains, respectively. Similarly, the biofilm formation capacity decreased by 27.12%, 33.98%, and 27.95% for the Δ*clpB*, Δ*lmo1438*, and Δ*lmo0294* gene deletion strains, respectively. The highest amount of biofilm formation was observed in the WT and gene deletion strains after 36 h of cultivation. During 36–72 h, the amount of biofilm formation gradually decreased, reaching the stage of biofilm shedding at 72 h, where some of the biofilm released planktonic bacteria.

3.8 The effect of key genes on motility

We evaluated the motility using the semisolid plate method between WT and gene mutant strains. The motility of ΔGL002291, ΔGL002712, Δ*clpB*, Δ*lmo1438*, and Δ*lmo0294* gene deletion mutant strains was significantly reduced compared to the WT when the incubation time reached both 36 and 72 h ($P < 0.05$, Fig. 10). Additionally, the motility of complementary strains was significantly enhanced compared to gene deletion mutant strains. After 72 h of incubation, the gene deletion mutant strains exhibited a significant difference in motility capacity compared to the WT ($P < 0.05$). The results illustrated that GL002291, GL002712, *lmo0294*, *clpB* and *lmo1438* play an important role in *L. monocytogenes*' motility.

3.9 The effect of key genes on the cell surface hydrophobicity and auto-aggregation

The cell surface hydrophobicity and auto-aggregation were measured to evaluate the effects of key genes on cell surface characteristics. The results showed that compared to the WT, the hydrophobicity of the ΔGL002291 and ΔGL002712 gene deletion strains exhibited no significant difference, however, the hydrophobicity of the Δ*lmo0294*, Δ*clpB*, and Δ*lmo1438* deletion strains decreased significantly (Fig. 11). The hydrophobicity of *lmo0294, clpB* and *lmo1438* complementary strains had no difference

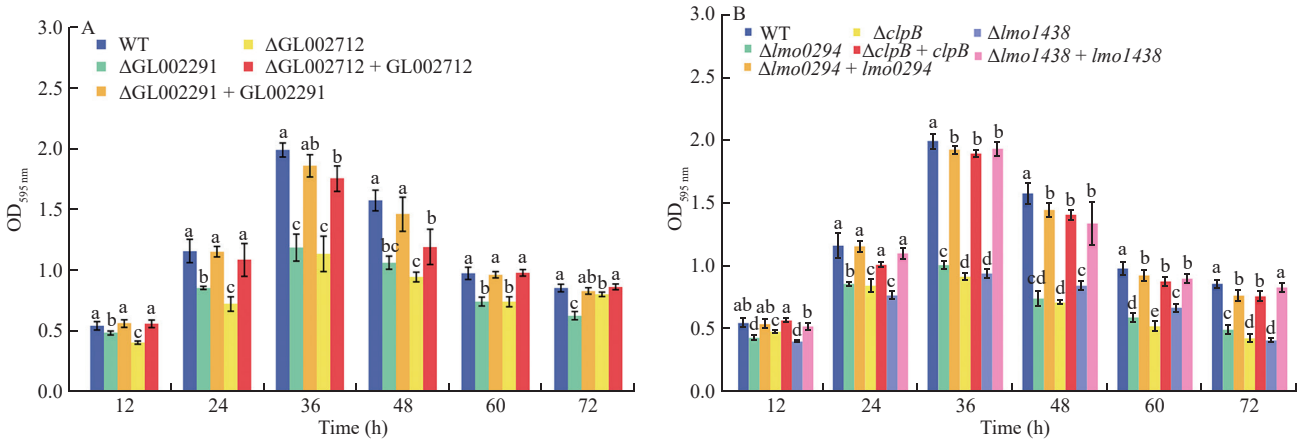

Fig. 9 Biofilm formation capacity of *L. monocytogenes* WT, gene deletion strains and complementary strains. (A) Gene deletion and complementation mutants of GL002291 and GL002712. (B) Gene deletion and complementation mutants of *clpB*, *lmo1438* and *lmo0294*. In the same groups, different lowercase letters represent significant difference ($P < 0.05$).

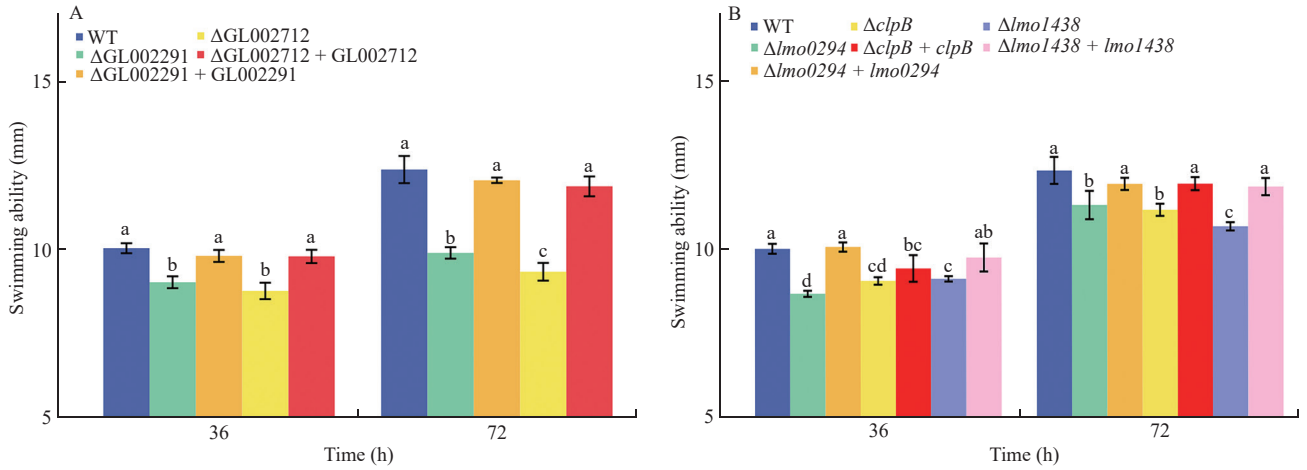

Fig. 10 Motility of *L. monocytogenes* WT, gene deletion strains and complementary strains. (A) Gene deletion and complementary strains of GL002291 and GL002712. (B) Gene deletion and complementary strains of *clpB*, *lmo1438*, *lmo0294*. In the same groups, different lowercase letters represent significant difference ($P < 0.05$).

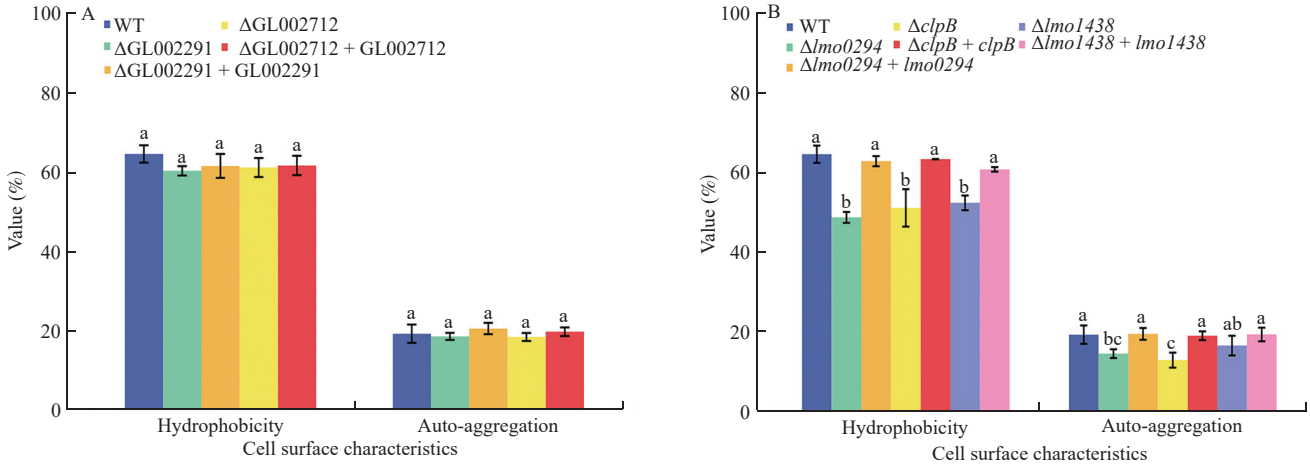

Fig. 11 Determination of cell surface hydrophobicity and auto-aggregation of *L. monocytogenes* WT, gene deletion strains and complementary strains. (A) Gene deletion and complementary strains of GL002291 and GL002712. (B) Gene deletion and complementary strains of *clpB*, *lmo1438* and *lmo0294*. In the same groups, different lowercase letters represent significant difference ($P < 0.05$).

compared with WT ($P > 0.05$). The data indicate that *lmo0294, clpB* and *lmo1438* regulates *L. monocytogenes* cell surface characteristics. Regarding auto-aggregation, the results showed that ΔGL002291 and ΔGL002712 gene deletion strains did not exhibit significantly different compared to the WT strain. However, the Δ*lmo0294*, Δ*clpB*, and Δ*lmo1438* gene deletion strains showed a significant decrease in auto-aggregation. Furthermore, the capacity of auto-aggregation was restored in the *lmo0294*, *clpB*, and *lmo1438* complementary strains. The results demonstrated that both hydrophobicity and cell auto-aggregation are associated with *lmo0294*, *clpB*, and *lmo1438*, and the cell surface characteristics affect biofilm formation.

4. Discussion

The presence of *L. monocytogenes* in food poses a serious health hazard. Additionally, biofilm enhances the resistance of *L. monocytogenes* to adverse conditions and causes persistent contamination. Therefore, it is important to investigate the potential regulatory genes in biofilm formation of *L. monocytogenes*. Although hydrophobicity and auto-aggregation are critical cell surface characteristics positively correlated with biofilm formation[20], studies have shown that there is no correlation between cell surface hydrophobicity and biofilm formation. This discrepancy may be attributed to differences in cell characteristics among different strains[18]. Our research illustrated that there was no significant difference in the capacity of hydrophobicity and auto-aggregation between LMB 33426 (a strong biofilm-forming strain) and CICC 21662 (a weak biofilm forming strain). Therefore, the difference in biofilm formation may not be attributed to cell surface characteristics between LMB 33426 and CICC 21662. Flagella plays an important role in motility of *L. monocytogenes*, regulated by temperature. Although flagella could not be detected on the surface of *L. monocytogenes*-EGDe when grown at 37 °C, individual differences in motility exist among different strains[21]. The LMB 33426 generated periplasmic flagella which contribute to the capacity of motility at 30 °C. We supposed that the difference in biofilm formation is attributed to the difference in the capacity of motility. The relationship between the capacity of motility and biofilm formation is not consistent. Previous research has shown that the flagella of *L. monocytogenes* are associated with initial adhesion and biofilm formation, and the biofilm formation capacity decreases with the loss of motility[16]. The motility of *L. monocytogenes* is negatively correlated with biofilm formation capacity in the mono-species biofilms and the dual-species biofilms[22]. Nevertheless, it has also been shown that flagellar mediated motility is essential for biofilm formation on abiotic surfaces, as the flagellar can overcome the repulsive forces during the initial adhesion stage[23]. In conclusion, there is a strain-specific relationship in *L. monocytogenes* between motility and biofilm formation.

The WGS and transcriptomics technologies has provided a vital method for screening of regulatory genes potentially involved in the biofilm formation. Genome sequencing techniques allow for the identification of important genetic characteristics[24]. Comparative genomics provides a deeper insight into the genomes and functional genes of strains, contributing to the identification of new mutations and the prediction of genes involved in biofilm formation[25].

The comparative genomic analysis identified two specific genes GL002291 and GL002712, which are associated with biofilm formation in LMB 33426. The ΔGL002291 and ΔGL002712 gene deletion mutant strains exhibited a significant decrease in both biofilm formation and motility in LMB 33426. According to the analysis conducted on NCBI, the GL002291 gene was found to encode a BglG family transcriptional anti-blocking factor. Abdelhamed et al.[12] identified BglG as a candidate virulence factor that controls the expression of sugar utilization genes. The Δ*bglG* gene deletion strains showed a reduction in the invasion of Caco-2 intestinal epithelial cells by *L. monocytogenes*. Furthermore, *bglG* may be involved in the host cell's response to carbohydrate perception and consumption during infection, contributing to pathogenesis[26]. Based on COG predictions, GL002291 is associated with signal transduction and carbohydrate transport and metabolism, which are known to regulate biofilm formation in *L. monocytogenes*[27]. On the other hand, the GL002712 gene encodes a glycosyltransferase which is associated with cell wall membrane components. A previous study showed that the operon of the *cdgL* gene carries a putative glycosyltransferase in *Bacillus thuringiensis*. The CdgL is predicted to be involved in membrane binding and regulation of motility, and the deletion of the *cdgL*

gene leads to the loss of flagellar structure and swimming motility[28]. It has also been shown that flagellin glycosylation affects the function of bacterial flagella[29], and inactivation of the glycosyltransferase gene *CD0240* results in the inability of bacteria to synthesize glycosylated flagellar filaments[30]. We suppose that the GL002712 gene as a glycosyltransferase is involved in flagellar synthesis in *L. monocytogenes*. The inactivation of the GL002712 gene in LMB 33426 led to a reduction in motility and positively regulated the capacity of biofilm formation.

The use of transcriptome sequencing technology may also contributes to the investigation of the regulatory mechanisms of biofilm formation[31]. Through comparative transcriptome analysis, the differentially expressed genes *clpB*, *lmo1438* and *lmo0294* were identified between planktonic and biofilm states in both LMB 33426 and CICC 21662. The deletion of Δ*clpB*, Δ*lmo1438*, and Δ*lmo0294* genes resulted in a significant reduction in the capacity of biofilm formation, motility, auto-aggregation, and hydrophobicity in *L. monocytogenes*. The auto-aggregation and hydrophobicity of cells are involved in the regulation of initial adhesion and biofilm formation[32]. The cell surface protein ClpS is responsible for the composition of the extracellular matrix, which is associated with bacterial adhesion to contact surfaces[33]. The ClpB protein are located on the cell surface and are essential for microbial stress responses. In *E. coli*, ClpB has been identified as heat shock protein for the growth and survival at high temperatures[34]. In *L. monocytogenes*, the *clpB* gene promoter binds to the stress regulator CtsR and the expression of the *clpB* gene is repressed by CtsR. The *clpB* has been identified as a regulator of virulence in *L. monocytogenes* in the regulation of various functional genes, including virulence, metabolism[35]. Additionally, the *clpB* gene participate in the biofilm formation, motility, and initial adhesion in the Gram-positive bacteria *B. amyloliquefaciens* FZB42[36], which supports the findings of this study. *Lmo1438* gene encodes a penicillin-binding protein that is involved in peptidoglycan assembly. Peptidoglycan precursors are synthesized in the cytoplasm and assembled on the cell surface by penicillin-binding proteins, among other proteins[37]. The absence of penicillin-binding proteins PBP1a and PBP1b impairs the capacity of biofilm formation in *E. coli*[38]. In *L. monocytogenes*, PBP4 is a transposon a penicillin-binding protein located on the cell membrane[39]. PBP4 mediates interactions with abiotic surfaces, and the deletion of PBP4 caused a decrease of the biofilm formation in *L. monocytogenes*[40]. The *lmo0294* gene belongs to the LysR transcription factor regulatory family. LysR transcription regulators can bind to the promoters of target genes and participation sensing and swimming properties[41].

5. Conclusions

In conclusion, our study involved a comprehensive comparative analysis of the WGS and transcriptome data to investigate genes associated with biofilm formation in *L. monocytogenes*. We identified specific genetic factors that may influence biofilm formation through their effects on motility and cell surface characteristics (Fig. 12). Future research should focus on conducting in-depth analyzes to elucidate the specific molecular pathways that regulate biofilm formation. Additionally, considering the importance of strain-specific responses in *L. monocytogenes*, future investigations could explore the diversity of genetic factors influencing motility and biofilm formation across different strains. Addressing these research gaps will not only advance our understanding of *L. monocytogenes* pathogenicity but also contribute to the development of targeted strategies for controlling biofilm-related infections.

Conflict of interest

The authors declare no conflict of interest.

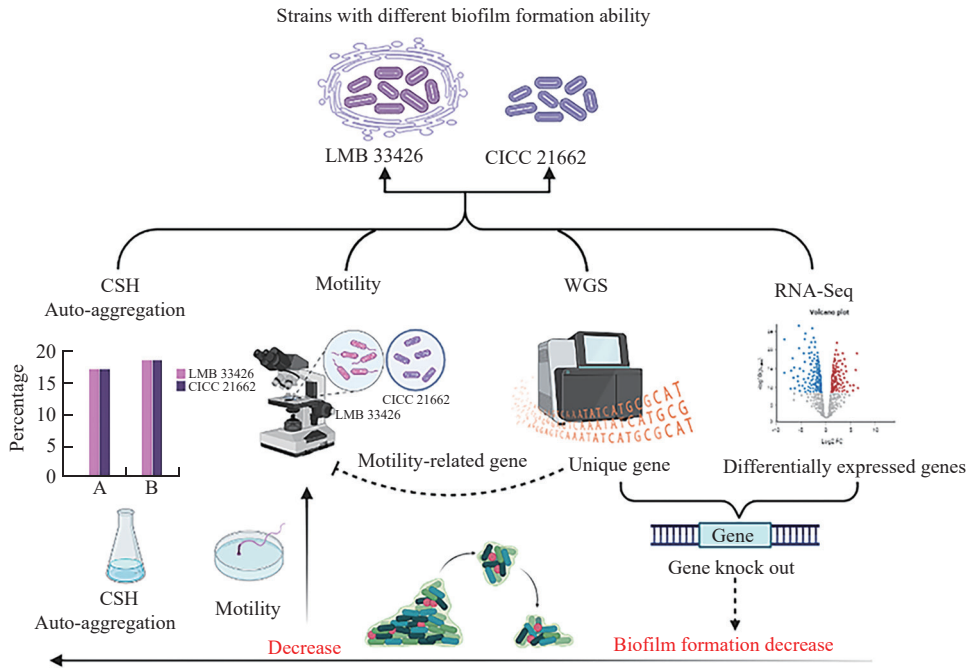

Fig. 12 Exploration of the causes of differences in biofilm formation. Figure generated with BioRender (https://biorender.com).

Acknowledgements

This research was financially supported by the National Natural Science Foundation of China (32272295), the Agricultural Independent Innovation Program in Jiangsu Province (CX(23)3043) and the Postgraduate Research & Practice Innovation Program of Jiangsu Province (KYCX23_0770).

Appendix A. Supplementary information

Supplementary data associated with this article can be found, in the online version, at http://doi.org/10.26599/FSHW.2024.9250297.

References

[1] Z. Fan, J. Xie, Y. Li, et al., Listeriosis in mainland China: a systematic review, Int. J. Infect. Dis. 81 (2019) 17-24. http://doi.org/10.1016/j.ijid.2019.01.007. Epub2019Jan11.

[2] Y.Y. Zhang, C. Zhou, A. Bassey, et al., Quantitative exposure assessment of cross-contamination from raw to ready-to-eat meat under different food-handling scenarios, Food Control 137 (2022) 108972. https://doi.org/10.1016/j.foodcont.2022.108972.

[3] C.N. Horita, R.C. Baptista, M.Y.R. Caturla, et al., Combining reformulation, active packaging and non-thermal post-packaging decontamination technologies to increase the microbiological quality and safety of cooked ready-to-eat meat products, Trends Food Sci. Technol. 72 (2018) 45-61. https://doi.org/10.1016/j.tifs.2017.12.003.

[4] J. Osek, B. Lachtara, K. Wieczorek, *Listeria monocytogenes*-how this pathogen survives in food-production environments? Front. Microbiol. 13 (2022) 866462. https://doi.org/10.3389/fmicb.2022.866462.

[5] E.M. Estrada, A.M. Hamilton, G.B. Sullivan, et al., Prevalence, persistence, and diversity of and species in produce packinghouses in three US states, J. Food Protect. 83 (2020) 277-286. https://doi.org/10.4315/0362-028X.JFP-19-411.

[6] P. Rodríguez-López, J.J. Rodríguez-Herrera, D. Vázquez-Sánchez, et al., Current knowledge on biofilms in food-related environments: incidence, resistance to biocides, ecology and biocontrol, Foods 7 (2018) 85. https://doi.org/10.3390/foods7060085.

[7] A. Colagiorgi, I. Bruini, P.A. Di Ciccio, et al., *Listeria monocytogenes* biofilms in the wonderland of food industry, Pathogens 6 (2017) 41. https://doi.org/10.3390/pathogens6030041.

[8] S.F. Oloketuyi, F. Khan, Inhibition strategies of *Listeria monocytogenes* biofilmscurrent knowledge and future outlooks, J. Basic Microbiol. 57 (2017) 728-743. https://doi.org/10.1002/jobm.201700071.

[9] P. Gerner-Smidt, J. Besser, J. Concepción-Acevedo, et al., Whole genome sequencing: bridging one-health surveillance of foodborne diseases, Front. Public Health 7 (2019) 172. https://doi.org/10.3389/fpubh.2019.00172.

[10] N. Unrath, E. Mccabe, G. Macori, et al., Application of whole genome sequencing to aid in deciphering the persistence potential of in food production environments, Microorganisms 9 (2021) 1856. https://doi.org/10.3390/microorganisms9091856.

[11] A. Casey, K. Jordan, A. Coffey, et al., Comparative genomic analysis of two serotype 1/2b *Listeria monocytogenes* isolates from analogous environmental niches demonstrates the influence of hypervariable hotspots in defining pathogenesis, Front. Nutr. 3 (2016) 54. https://doi.org/10.3389/fnut.2016.00054.

[12] H. Abdelhamed, M.L. Lawrence, R. Ramachandran, et al., Validation of predicted virulence factors in *Listeria monocytogenes* identified using comparative genomics, Toxins 11 (2019) 2509-2545. https://doi.org/10.1080/21505594.2021.1975526.

[13] A. Lamas, P. Regal, B. Vázquez, et al., *Salmonella* and *Campylobacter* biofilm formation: a comparative assessment from farm to fork, J. Sci. Food Agric. 98 (2018) 4014-4032. https://doi.org/10.1002/jsfa.8945.

[14] Q. Luo, J.L. Shang, X.Q. Feng, et al. PrfA led to reduced biofilm formation and contributed to altered gene expression patterns in biofilm-forming, Curr. Microbiol. 67 (2013) 372-378. https://doi.org/10.1007/s00284-013-0377-7.

[15] C. Rodríguez-Melcón, C. Alonso-Calleja, R. Capita, Architecture and viability of the biofilms formed by nine *Listeria* strains on various hydrophobic and hydrophilic materials, Appl. Sci. 9(23) (2019) 5256. https://doi.org/10.3390/app9235256.

[16] Y. Fan, J. Qiao, Z. Lu, et al., Influence of different factors on biofilm formation of *Listeria monocytogenes* and the regulation of *cheY* gene, Food Res. Int. 137 (2020) 109405. https://doi.org/10.1016/j.foodres.2020.109405.

[17] L.N. Wei, C.Z. Shi, C.X. Luo, et al., Phloretin inhibits biofilm formation by affecting quorum sensing under different temperature, LWT-Food Sci. Technol. 131 (2020) 109668. https://doi.org/10.1016/j.lwt.2020.109668.

[18] J. Woo, J. Ahn, Probiotic-mediated competition, exclusion and displacement in biofilm formation by food-borne pathogens, Lett. Appl. Microbiol. 56 (2013) 307-313. https://doi.org/10.1111/lam.12051.

[19] X.B. Jiang, S.Y. Ren, Y.M. Geng, et al., Role of the VirSR-VirAB system in biofilm formation of *Listeria monocytogenes* EGD-e, Food Res. Int. 145 (2021) 11039. https://doi.org/10.1016/j.foodres.2021.110394.

[20] N.Y. Choi, Y.M. Bae, S.Y. Lee, Cell surface properties and biofilm formation of pathogenic bacteria, Food Sci. Biotechnol. 24 (2015) 2257-2264. https://doi.org/10.1007/s10068-015-0301-y.

[21] A. Gründling, L.S. Burrack, H.G.A. Bouwer, et al., *Listeria monocytogenes* regulates flagellar motility gene expression through MogR, a transcriptional repressor required for virulence, Proc. Nat. Acad. Sci. 101 (2004) 12318-12323. https://doi.org/10.1073/pnas.0404924101.

[22] Q. Dong, L. Sun, T. Fang, et al., Biofilm formation of *Listeria monocytogenes* and *Pseudomonas aeruginosa* in a simulated chicken processing environment, Foods 11(13) (2022) 1917. https://doi.org/10.3390/foods11131917.

[23] I. Doghri, T. Cherifi, C. Goetz, et al., Counteracting bacterial motility: a promising strategy to narrow biofilm in food processing industry, Front. Microbiol. 12 (2021) 673484. https://doi.org/10.3389/fmicb.2021.673484.

[24] A. Ben Hassena, J. Haendiges, S. Zormati, et al., Virulence and resistance genes profiles and clonal relationships of non-typhoidal food-borne strains isolated in Tunisia by whole genome sequencing, Int. J. Food Microbiol. 337 (2021). https://doi.org/10.1016/j.ijfoodmicro.2020.108941.

[25] D. Wang, G.C. Fletcher, D. Gagic, et al., Comparative genome identification of accessory genes associated with strong biofilm formation in *Vibrio parahaemolyticus*, Food Res. Int. 166 (2023) 112605. https://doi.org/10.1016/j.foodres.2023.112605.

[26] F.M. Rothe, T. Bahr, J. Stülke, et al., Activation of antiterminator BglG requires its phosphorylation, Proc. Nat. Acad. Sci. 109 (2012) 15906-15911. https://doi.org/10.1073/pnas.1210443109.

[27] J. Gray, P.S. Chandry, M. Kaur, et al., Colonisation dynamics of *Listeria monocytogenes* strains isolated from food production environments, Sci. Rep. 11 (2021) 12195. https://doi.org/10.1038/s41598-021-91503-w.

[28] V. Smith, I.K.B. Nilssen, I.K. Hegna, et al., CdgL is a degenerate nucleotide cyclase domain protein affecting flagellin synthesis and motility in *Bacillus thuringiensis*, Res. Microbiol. 172 (2021) 103850. https://doi.org/10.1016/j.resmic.2021.103850.

[29] B. Janesch, F. Schirmeister, D. Maresch, et al., Flagellin glycosylation in *Paenibacillus alvei* CCM 2051T, Glycobiology 26 (2016) 74-87. https://doi.org/10.1093/glycob/cwv087.

[30] S.M. Twine, C.J. Paul, E. Vinogradov, et al., Flagellar glycosylation in *Clostridium botulinum*, FEBS J. 275 (2008) 4428-4444. https://doi.org/10.1111/j.1742-4658.2008.06589.x.

[31] O.E. Petrova, F. Garcia-Alcalde, C. Zampaloni, et al., Comparative evaluation of rRNA depletion procedures for the improved analysis of bacterial biofilm and mixed pathogen culture transcriptomes, Sci. Rep. 7 (2017) 41114. https://doi.org/10.1038/srep41114.

[32] Y. Wang, L.P. Samaranayake, G.A. Dykes, Tea extracts modulate oral biofilm development by altering bacterial hydrophobicity and aggregation, Archives of Oral Biology, 122 (2021) 105032. https://doi.org/10.1016/j.archoralbio.2020.105032.

[33] X. Zhao, Y. Wang, Q.H. Shang, et al., Collagen-like proteins (ClpA, ClpB, ClpC, and ClpD) are required for biofilm formation and adhesion to plant roots by FZB42, PLoS ONE 10 (2015) e0117414. https://doi.org/10.1371/journal.pone.0117414.

[34] S. Kedzierska-Mieszkowska, M. Zolkiewski, Hsp100 molecular chaperone Clpb and its role in virulence of bacterial pathogens, Int. J. Mol. Sci. 22 (2021) 5319. https://doi.org/10.3390/ijms22105319.

[35] A. Chastanet, I. Derre, S. Nair, et al., ClpB, a novel member of the *Listeria monocytogenes* CtsR regulon, is involved in virulence but not in general

stress tolerance, J. Bacteriol. 186 (2004) 1165-1174. https://doi.org/10.1016/S0377-8401(97)00070-9.

[36] X. Zhao, R.Y. Wang, Q.H. Shang, et al., The new flagella-associated collagen-like proteins ClpB and ClpC of *Bacillus amyloliquefaciens* FZB42 are involved in bacterial motility, Microbiol. Res. 184 (2016) 25-31. https://doi.org/10.1016/j.micres.2015.12.004.

[37] N. Janez, B. Skrlj, M. Sternisa, et al., The role of the *Listeria monocytogenes* surfactome in biofilm formation, Microb. Biotechnol. 14 (2021) 1269-1281. https://doi.org/10.1111/1751-7915.13847.

[38] A. Kumar, S.K. Sarkar, D. Ghosh, et al., Deletion of penicillin-binding protein 1b impairs biofilm formation and motility in *Escherichia coli*, Res. Microbiol. 163 (2012) 254-257. https://doi.org/10.1016/j.resmic.2012.01.006.

[39] J. Zawadzka-Skomial, Z. Markiewicz, M. Nguyen-Distéche, et al., Characterization of the bifunctional glycosyltransferase/acyltransferase penicillin-binding protein 4 of *Listeria monocytogenes*, J. Bacteriol. 188 (2006) 1875-1881. https://doi.org/10.1128/JB.188.5.1875-1881.2006.

[40] Y.H. Chang, W.M. Gu, N. Fischer, et al., Identification of genes involved in *Listeria monocytogenes* biofilm formation by mariner-based transposon mutagenesis, Appl. Microbiol. Biotechnol. 93 (2012) 2051-2062. https://doi.org/10.1007/s00253-011-3719-z.

[41] H. Abdelhamed, R. Ramachandran, L. Narayanan, et al., Contributions of a LysR transcriptional regulator to *Listeria monocytogenes* virulence and identification of its regulons, J. Bacteriol. 202 (2020) e00087-20. https://doi.org/10.1128/JB.00087-20.